Petroleum & Coal
ISSN 1337-7027

Available online at www.vurup.sk/petroleum-coal
Petroleum & Coal 57(6) 609-618, 2015

A MATHEMATICAL MODEL TO DESIGN MERCAPTANS REMOVAL UNIT (MRU) USING REAL COMPONENT LUMPING APPROACH

Saeed Khademi[1], Hossein Anisi[1], Sajad Mirian[1], Xiang Yu[2], Sepehr Sadighi[3*]

[1]Molecular Sieve Division, Nitelpars Co. (Fateh Group), Tehran, Iran; [2]Application Engineer of Hengye Molecular Sieve Co., Shanghai, China; [3]Catalysis Research Division, Research Institute of Petroleum Industry (RIPI), Tehran, Iran

Received October 19, 2015, Accepted December 14, 2015

Abstract

Environmental legislations force natural gas refineries to purify their products to less than 10 ppmv of sulfur content. To commercially do such a criterion, adsorption process is the first option for removing sulfur compounds especially H_2S and mercaptans from gaseous streams. Due to the importance of accurate and robust design of such facilities, in this research, a fundamental model is proposed to calculate the breakthrough and regeneration time of an industrial scale temperature swing adsorption (TSA) process. This facility is specifically designed for removing mercaptans from natural gas which is called mercaptans removal unit (MRU). Results show that the time length of the adsorption and regenerations steps estimated by the MRU model are 20.5 and 11 hours, respectively, close to the obtained values from the industrial scale plant (18 and 12 hours, respectively). Therefore, during the process design, the actual cycle time can be considered about 10% less than the value estimated by the model. Additionally, it is demonstrated that increasing the flow rate of the regeneration stream (about 35% higher than design value) decreases the regeneration time about 12% which can be an option to shorten the duration of regeneration step, but its effect on the downstream units, especially sulfur recovery unit (SRU) should be evaluated.

Keywords: Adsorption; Mercaptan; Model; Zeolite 13X.

1. Introduction

Natural gas (NG) stream contains impurities such as water vapor, carbon dioxide, hydrogen sulfide, and light mercaptans. Due to the environmental legislation and corrosion problems, sulfur components of NG must be removed to less than 10 ppmv, before sending to the pipelines. Common desulfurization processes like amine treatment could not reduce the sulfur content at this level to meet the desired standard [1,2]. In amine-wash unit, most acid gases such as CO_2 and H_2S are removed from NG, though light mercaptans which are not acidic could not be completely separated from process stream, and therefore, a secondary process is needed to remove such compounds [3]. In last few years, several works in the field of adsorption on different types of zeolites have been reported [4-10]. Accordingly, adsorption can be divided into three main groups based on applied regeneration procedure i.e. decreasing partial pressure (pressure swing adsorption or PSA), creating vacuum (vacuum swing adsorption or VSA), and increasing temperature (temperature swing adsorption or TSA) [11]. It can be found that this process proposed by Khale for air-drying in 1942, has been significantly improved in comparison to the other separation processes such as cryogenic distillation [12].

In adsorption process, after adsorption, the adsorbed impurities must be removed in the regeneration step. In TSA process, a hot gas or treated product is used for regenerating the bed, and after that, the bed is usually cooled down by a cold gas stream before starting

adsorption step [13]. A large number of modeling and simulation works using different types of adsorbents are available in literature. La Cava et al. [14] and Dasilva et al. [15] proposed models to predict the parameters of adsorption units. Kim et al. [16] studied a six-step PSA system using carbon molecular sieve (CMS) to produce O_2 with high purity, and also to study the performance of PSA unit under non-isothermal condition. Knaebel et al. simulated and optimized PSA unit to maximize the hydrogen recovery and also the purity of product [17]. Shirani et al. proposed a model for adsorption process utilized for removing mercaptans and water from NG using 13X zeolite under isothermal condition. In this model, the rate of adsorption was approximated by linear driving force (LDF) expression, and the extended Langmuir isotherm was used to describe adsorption equilibrium [18]. Cho et al. [19] investigated the use of pressure-temperature swing adsorber (PTSA) for separation of green gas SF6 from a mixture of N_2 using activated carbon. In this study, the maximum purity of 19.5% and recovery of 50.1% obtained with adsorption pressure and temperature of 2.5 atm and 200°C, respectively. Mulgundmath and Tazel [20] compared PSA with TSA for recovery of CO_2 from the flue gas using Ceca 13X adsorbent, and therefore, cyclic adsorption process was optimized. Taheri et al. simulated PTSA process for two-layer six bed adsorption system to remove mercaptans from NG. They suggested some changes to upgrade the design conditions for sake of energy saving without affecting the purification performance [21].

In this research, a TSA system to remove mercaptans from NG using the 13X molecular sieve has been studied. The main objective of this work is to propose a fundamental model to estimate the breakthrough and regeneration time for an industrial scale mercaptans removal unit (MRU) based on real component lumping approach. Additionally, as a key parameter, the content of mercaptans in the regeneration gas is studied.

2. Process description

The target adsorption unit consists of six insulated beds which are designed for purifying NG, and removing impurities such as water vapor and mercaptans. Each bed includes two layers which are 13X zeolite as the main bed, and activated alumina as the guard bed. The latter is specifically used for the protection of 13X zeolite from water. Specifications of adsorbents and beds are presented in Table 1.

Table1 Adsorbents specification and bed configuration

Parameter	Zeolite 13X	Activated alumina
Bed Configuration		
Bed length (m)	4.65	0.75
Bed diameter (m)	3.75	3.75
Adsorbents specification		
Shape	Beads	Beads
Particle radius (mm)	2.38-3.36	3.0-4.0
Bulk density (g/cm^3)	0.66	0.74

Table 2 Design specifications –natural gas, regeneration gas flow for each step 8.2987 kg/h

Stages	Characteristics	Value
Adsorption Stage	Pressure (bar)	68
	Temperature (°C)	40
	Time duration (h)	18
	Flow direction	Top to bottom
Heating Stage	Pressure (bar)	12
	Temperature (°C)	320
	Time duration (h)	12
	Flow direction	Bottom to top

Table 2 (contd.) Design specifications –natural gas, regeneration gas flow for each step 8.2987 kg/h

Stages	Characteristics	Value
Cooling Stage	Pressure (bar)	12
	Temperature (°C)	38
	Time duration (h)	4
	Flow direction	Bottom to top

Table 3 Feed specification of MRU

Feed Operating Conditions		
Specification	Unit	Value
Temperature	°C	40
Pressure	bar	68
Total Flow rate	(kg/h)	471,374
Feed Composition		
Methane	mol%	86.33
Ethane	mol%	5.46
Propane	mol%	2.17
CO_2	mol%	1.33
i-Butane	mol%	0.3785
n-Butane	mol%	0.5125
i-Pentane	mol%	0.1088
N-Hexane	mol%	0.023
Benzene	mol%	0.001
Total Mercaptan	mol%	0.0134
Water	mol%	0.0018

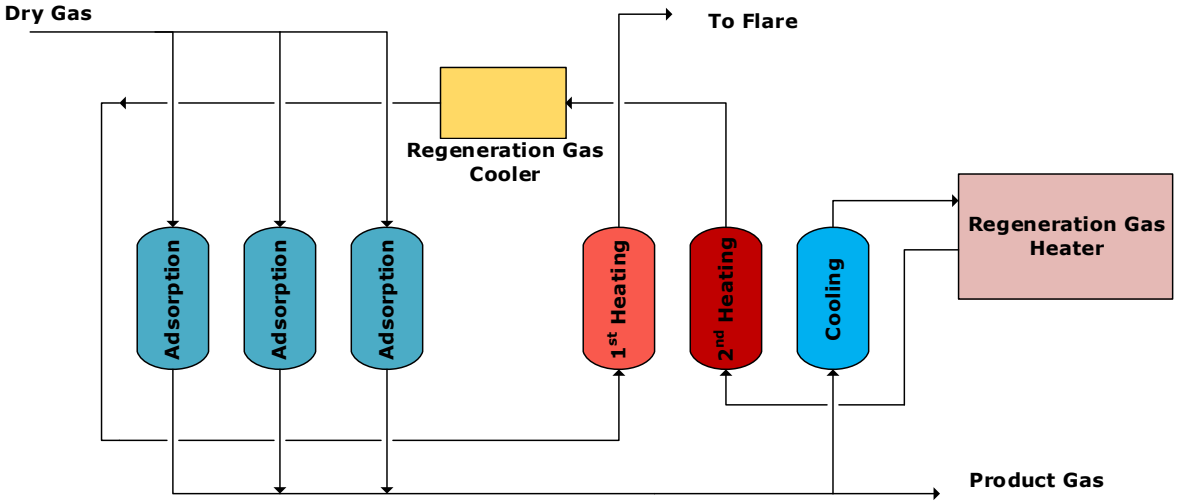

Figure 1. Schematic diagram of mercaptans removal unit (MRU)

3. Material and method

The following assumptions are used to model the MRU:

- The gas phase is ideal.
- Because activated alumina is located at the top of 13X molecular sieve, the water content of the natural gas during adsorption process is negligible.
- A DPCU (dew point control unit) has been placed at the upstream of MRU. Therefore, the problem of aromatic and heavy hydrocarbons are alleviated [22].
- According to Table 3, feed is lumped to methane (86.33 mol %), propane (13.67 mol%), and methyl mercaptans (0.01366 mol%).

- The bed operates in isothermal condition without any heat transfer between solid and gas phase.
- The bed void is initially filled with methane.
- According to the literature [21], the temperature variation along the MRU bed is only observed at a short time after starting the regeneration step. To simplify the model for design purposes, the temperature along the bed is assumed constant.
- Only axial mass dispersion is considered.
- Pressure gradient is related to the superficial velocity, and is calculated by Ergun equation.
- Mass transfer coefficients consist of film resistance and macro pore diffusion.

These assumptions have been widely accepted by numerous adsorption studies [23-25]. Accordingly, the general and particular equations are written as follows.

3.1 General equations

3.1.1 Momentum balance

In this study, bed dimensions and particle diameter are constant; therefore, based on Ergun's equation, the superficial velocity can be related to the total pressure gradient as follows [26,32]:

$$\frac{\partial p}{\partial z} = -\left(\frac{1.5\times10^{-3}(1-\varepsilon)^2}{(2r_p\psi)^2\,\varepsilon^3}\mu v_g + 1.75\times10^{-5}M\rho_g\frac{(1-\varepsilon)}{2r_p\psi\,\varepsilon^3}{v_g}^2\right) \quad (1)$$

Ergun equation considers laminar and turbulent flow conditions to calculate the pressure drop across the bed.

3.1.2 Material balance

The mass balance in the gas phase depends on the effect of axial dispersion, convection term, gas phase accumulation, and the rate of fluid to the adsorbent as follows [27,28,32]:

$$-\varepsilon D_{ax}\frac{\partial^2 c_i}{\partial z^2} + v_g\frac{\partial(c_i)}{\partial z} + \frac{\partial c_i}{\partial t} + \frac{1-\varepsilon}{\varepsilon}\frac{\partial \bar{q}_i}{\partial t} = 0 \quad (2)$$

The dispersion coefficient in Eq.2 is calculated from the following correlation [23-26,32]:

$$D_{ax} = 0.73D_{mi} + \frac{v_g r_p}{\varepsilon(1+9.49\frac{\varepsilon D_{mi}}{2v_g r_p})} \quad (3)$$

Moreover, to calculate binary molecular diffusivity (D_{AB}), Fuller, Schettler and Giddings equation is used. This equation includes empirical constants and keeps the form of Chapman-Enskog kinetic theory [29,32].

$$D_{AB} = \frac{0.00143T^{1.75}}{PM_{AB}^{1/2}[(\Sigma_v)_A^{1/3} + (\Sigma_v)_B^{1/3}]^2} \quad (4)$$

3.2 Particular equations

3.2.1 Kinetic model

Mass transfer driving force is assumed to be a linear function of solid. Therefore, it consists of two terms as follows [30-32]:

- Extra-particle transport mechanisms
- Intra-particle transport mechanisms

The overall mass transfer coefficient can be calculated as the following:

$$\frac{1}{k_{MTC_i}} = \frac{r_p\bar{K}_{ki}}{3k_{fi}} + \frac{r_p^2\bar{K}_{ki}}{15\varepsilon_p D_{pi}} \quad (5)$$

In extra-particle transport term the film resistance is estimated from Sherwood number

and Wakao-Funazkri correlation as the following [30-32]:

$$k_{fi} = sh_i \frac{D_{mi}}{2r_p} \quad (6)$$

$$sh_i = 2.0 + 1.1Sc_i^{1/3} Re^{0.6} \quad (7)$$

Above correlation is reliable in the Reynolds number between 3 and 104 [31,32].

For the intra-particle transport term, the macro pore diffusion includes both molecular and Knudsen diffusions which can be calculated from the Bosanquet equation as follows [30-32]:

$$\frac{1}{D_{pi}} = \tau\left(\frac{1}{D_{ki}} + \frac{1}{D_{mi}}\right) \quad (8)$$

$$D_{ki} = 97 r_{pore}\left(\frac{T}{M_i}\right)^{0.5} \quad (9)$$

where τ is the tortuosity factor and is dependent to the porosity as follows [31]:

$$\tau = \varepsilon_p + 1.5(1 - \varepsilon_p) \quad (10)$$

3.2.2 Isotherm model

The relationship between loading of molecular sieve and the partial pressure or concentration of adsorbate is known as isotherm curve. The Langmuir-type isotherm is the most relevant model for practical applications. In this research, the Langmuir isotherm for pure component adsorption is used. Details for estimating the isotherm parameters were described in the previous work [32]. The isotherm parameters which were used in this work were reported by Hengye Molecular Sieve Company.

3.3 Numerical solution

All of the mentioned equations are solved using Aspen Custom Modeler (ACM) software (Aspen Tech, 2013) with appropriate initial and boundary conditions to estimate the breakthrough time of the target TSA system. In this software, to solve the partial differential equations, at first they are transferred to ordinary differential equations (ODEs) using method of lines. Then, these ODEs are solved numerically using the Implicit Euler integrator.

4. Results and discussion

By numerically solving Equations (1) & (2) in ACM flowsheet using the mentioned assumptions and equations, MRU was simulated. Then, the mercaptans content of both NG product and outlet regeneration stream were obtained.

Figure 2 shows the breakthrough curve of the target MRU. As seen, before t=43000 sec (about 12 h), the mercaptan content of the product is less than 0.1 ppmv. After that, mercaptans impurity sharply increases with time. It can be observed that at the time=74000 sec (about 20.5 h), the mercaptan content of the product increases to higher than 10 ppmv which is the most tolerable value for mercaptans content of NG (the standard level is lower than 10 ppmv).

According to observations from industrial scale process, the adsorption time of each cycle for removing mercaptans from NG using 13X molecular sieve is about 18 h. It can be concluded that obtained result is fairly close to this value. However, the higher cycle time is mainly due to the Langmuir parameters estimated from the static experiments. The dynamic capacity of molecular sieves is usually lower than the static value, so the lower cycle time is expectable. According to these results, the cycle time of the real plant should be considered about 10% less than the value obtained from the MRU model.

In Figure 3, the weight fraction of mercaptans in the outlet stream of the bed during regeneration process is presented (at the design flow rate=8878 kg/h). As seen, at the start of the regeneration step (t=74000 sec), mercaptans content of the regeneration stream sharply increases such that at t=78000 sec (about 2 h after starting regeneration step), the concentration of mercaptans reaches to about 26500 ppmv. Moreover, a peak for

mercaptans content of this stream can be seen. It can be concluded that during the regeneration cycle, mercaptans removal is not even. This phenomenon affects the sulfur recovery unit (SRU) as the catalyst of that is designed for a certain mercaptan level, and it is very sensitive to mercaptans load changes [33].

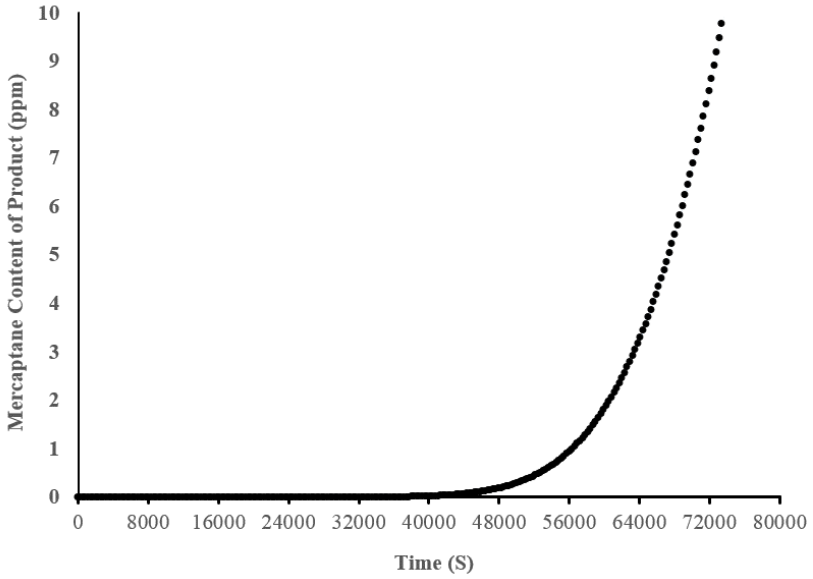

Figure 2. Mole fraction of mercaptans versus time in the natural gas product

To find the sensitivity to the regeneration flow rate, this value is set to 12000 kg/h, the highest accessible value for the flow rate of regeneration stream. As shown in Fig.3, by increasing that, the regeneration time decreases without showing any effect on the peak level. However, at the higher flow rate, the area of mercaptans removal is broader, so the downstream unit should be designed to tolerate this excess loading.

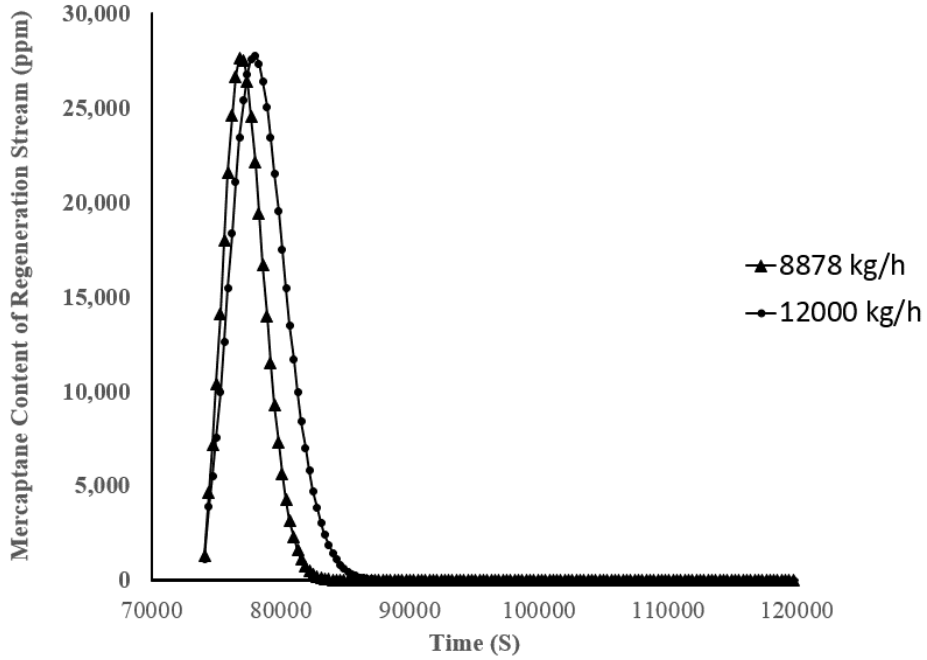

Figure 3 Mole fraction of mercaptans versus time in the gas stream during regeneration

Figures 4 and 5 indicate the mercaptan content of the regeneration stream at the design and overdesigned flow rates during the end of the step. As seen in Figure 4, the bed is completely regenerated at t=114000 sec (about 31.5 h) when the stream flow rate is 8878 kg/h. Therefore, the regeneration time (heating) about 11 h is enough to remove mercaptans from the surface of the adsorbent. According to the industrial observation, heating time about 12 h is recommended for this type of molecular sieve. Furthermore, Figure 5 confirms that increasing the regeneration stream (from 8878 to 12000 kg/h) decreases the regeneration time (from 114000 sec to 102000 sec) which can be an option to shorten the regeneration step. But, its influence on the downstream unit (i.e., SRU) should be considered.

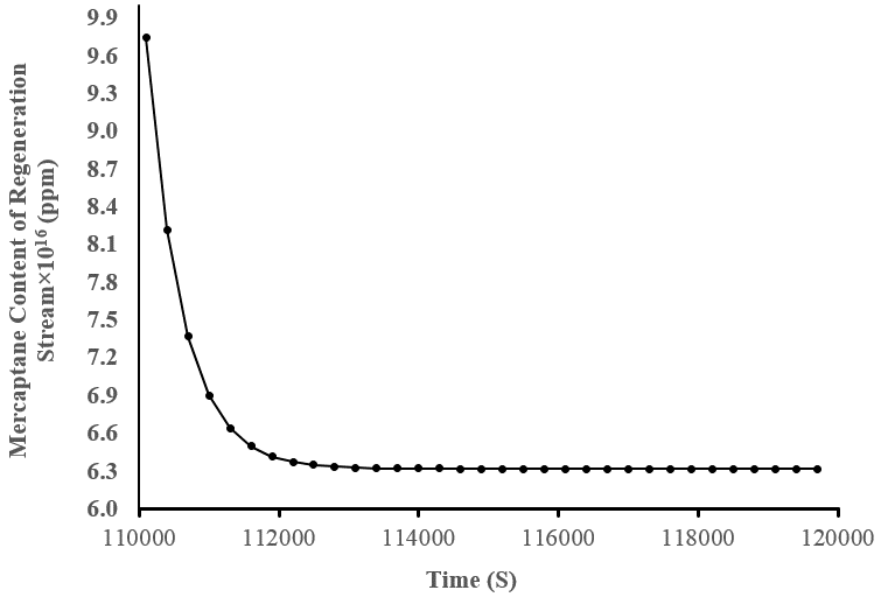

Figure 4 Mole fraction of mercaptans versus time at the end of the regeneration
Regeneration rate=8878 kg/h

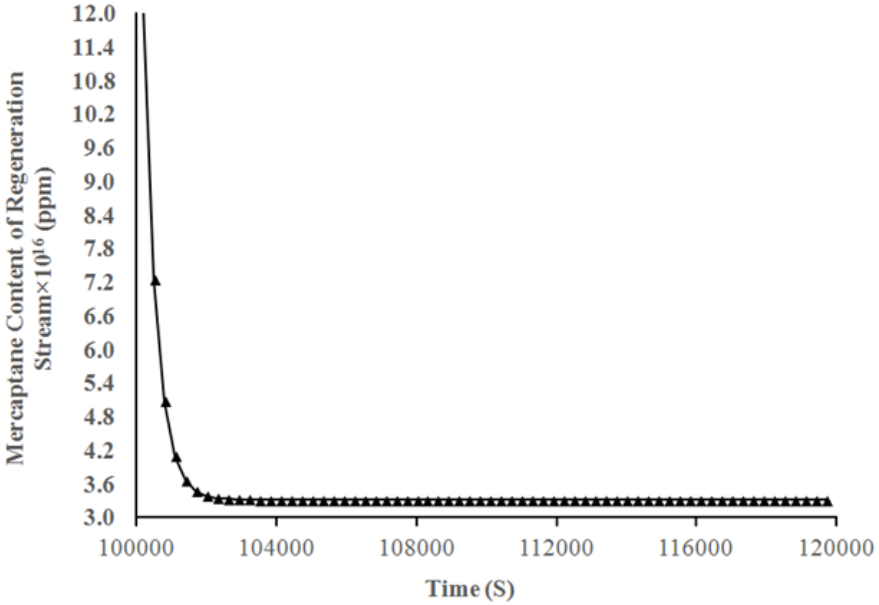

Figure 5 Mole fraction of mercaptans versus time at the end of the regeneration
Regeneration rate=12000 kg/h

5. Conclusion

To study the performance of adsorption units, many models are available in open literature. But, in this survey, a fundamental model according to the real component lumping approach was proposed to predict the momentous process variables of MRU i.e. adsorption and regeneration cycle length. Moreover, this model was capable of analyzing the sensitivity of the process to the feed and regeneration flow rates.

Results showed that at design conditions, 12 hours after starting the adsorption step, the mercaptans content of the product was still lower than 0.1 ppmv. After this period, mercaptans content of the product rise up versus time, and about 8.5 hours later, it reached to10 ppmv (maximum allowed value for sulfur compounds).

Additionally, it was found that about 2 h after starting regeneration step, mercaptans content of the outlet regeneration gas stream sharply reached to the highest possible value (i.e. 26500 ppmv). The amount of mercaptans in the regeneration off-gas varied according to the molecular sieve regeneration cycle, which then required overdesign of some items of the downstream facilities especially Claus unit. It was confirmed that increasing the flow rate of regeneration stream decreased the regeneration time without influencing the mercaptans peak level. But, at the higher values, mercaptans removal area was broader, and therefore, the downstream unit should tolerate this extra burden.

Because the adsorption and regeneration times estimated by the model (20.5 and 11 hours, respectively) were close enough to the observed actual values (18 and 12 hours, respectively), the proposed MRU model based on real component lumping approach could be a reliable tool for the design purposes.

Nomenclature

P	*Pressure (atm)*	k_{MTC_i}	*Mass transfer coefficient (1/s)*
T	*Temperature (K)*	k_{fi}	*Film resistance coefficient (1/s)*
Σ_v	*Summation of atomic diffusion Volume*	ε_p	*Particle porosity*
ε	*Bed void fraction*	D_{pi}	*Macro pore diffusion coefficient (cm^2/s)*
r_p	*Particle radius (m)*	sh	*Sherwood number*
r_{pore}	*Pore radius (m)*	D_{mi}	*Gas mixtures molecular diffusion (cm^2/s)*
$\overline{K}_{ki}$	*Henry Coefficient*	Sc	*Schmidt number*
ψ	*Shape factor*	Re	*Reynolds number*
μ	*Dynamic viscosity (Pa.s)*	τ	*Tortuosity factor*
υ_g	*Superficial velocity (m/s)*	D_{ki}	*Knudsen diffusion (cm^2/s)*
M	*Molecular weight*	q_i	*Loading of component i (kmol/kg adsorbent)*
ρ_g	*Gas density (kg/m^3)*	IP	*Isotherm parameter*
D_{ax}	*Axial dispersion coefficient (cm^2/s)*	p_i	*Partial pressure of component i*
ρ_b	*Solid bulk density (kg/m^3)*		

Acknowledgements

We would like to express our great appreciation to Mr. F. Noorbakhsh, Mr. A. Tavangar and Dr. M. A. Fatemi for their valuable and constructive suggestions during the planning and development of this research work. We would also like to thank Nitel Pars Company a subsidiary of Fateh Group for the financial support, and Hengye Molecular Sieve Company for the technical assistance.

References

[1] Weber G, Bellat JP, Benoit F, Paulin C. Adsorption Equilibrium of Light Mercaptans on Faujasites. Adsorption 2005; 11: 183-188.

[2] Weber G, Benoit F, Bellat JP, Paulin C, Mougin P, Thomas M. Selective adsorption of ethyl mercaptan on NaX zeolite. Microporous and Mesoporous Materials. 2008; 109:184-192.

[3] Weber G, Benoit F, Bellat JP, Paulin C, Mougin P, Thomas M. Adsorption equilibria of binary ethylmercaptan/hydrocarbon mixtures on a NaX zeolite. Adsorption 2008;14:501-507.
[4] Garcia C, Lercher J. Adsorption and surface chemistry of light thiols on Na-ZSM5 and H-ZSM5 J. Phys. Chem. 1991;95:10729-10736.
[5] Sakano T, Yamamura K, Tamon H, Miyahara M, Okazaki M. Improvement of Coffee Aroma by Removal of Pungent Volatiles Using A-Type Zeolite. Journal of Food Science 1996;61:473-476.
[6] Sarbak Z. Desulfurization of ethanethiol over cadmium and mercury modified zeolite NaX. Applied Catalysis A: General 1996;147:47-54.
[7] Sarbak Z. Elimination of Odours from the Gaseous Phase on CrIII And FeIII-Modified Y-Type Zeolites. Adsorption Science Technology 2001;19:187-195.
[8] Maldonado H, Yang RT. Desulfurization of liquid fuels by adsorption via π complexation with Cu(I)-Y and Ag-Y zeolites. Ind. Eng. Chem 2003;42:123-129.
[9] Wakita H, Ono Y, Tachibana Y, Hosaka M. Method for removing sulfur compound present in city gas. 2003.
[10] Maldonado H, Stamatis SD, Yang RT, He AZ, Cannella W. New sorbents for desulfurization of diesel fuels via p complexation: layered beds and regeneration. nd. Eng. Chem. 2004;43:769-776.
[11] Cruz P, Santos JC, Magalhaes FD, Mendes A. Cyclic adsorption separation processes: analysis strategy andoptimization procedure. Chemical Engineering Science. 2003;58:3143-3158.
[12] Espitalier-Noel P. Waste recycle pressure swing adsorption to enrich oxygen from air. Ph.D., University of de Surrey, UK. 1998.
[13] Clausse JBM, Meunier F. Adsorption of gas mixtures in TSA adsorbers under various heat removal conditions. Chemical Engineering Science 2004;59:3657-3670.
[14] La Cava Al, Domingues JA, Cardenas J. Modeling and simulation of rate induced PSA separations. Adsorption: Science and technology 1989;158:323.
[15] Da Silva FA, Silva JA, Rodrigues AE. A General Package for the Simulation of Cyclic Adsorption Processes. Adsorption. 1999;5:229-244.
[16] Kim MB, Jee JG, Bae YS, Lee CH. Parametric Study of Pressure Swing Adsorption Process To Purify Oxygen Using Carbon Molecular Sieve. Ind. Eng. Chem. Res 2005;44:7208-7217.
[17] Seth DK, Knaebel P, Biegler LT. Simulation and Optimization of a Pressure Swing Adsorption System: Recovering Hydrogen from Methane. Adsorption 2005;11:615-620.
[18] Shirani B, Kaghazchi T, Beheshti M. Water and mercaptan adsorption on 13X zeolite in natural gas purification process. Korean Journal of Chemical Engineering 2010;27:253-260.
[19] Wan S.C., Lee K.H., Chang H.J., Huh W., Kwon H.H. Evaluation of pressure-temperature swing adsorption for sulfur hexafluoride (SF6) recovery from SF6 and N2 gas mixture. Korean Journal of Chemical Engineering 2011;28: 2196-2201.
[20] Mulgundmath TV, Tezel FH. Optimisation of carbon dioxide recovery from flue gas in a TPSA system. Adsorption 2010;16: 587-598.
[21] Taheri Qazvini O, Fatemi S. Modeling and simulation pressure–temperature swing adsorption process to remove mercaptan from humid natural gas; a commercial case study. Separation and Purification Technology 2015; 88-103.
[22] Mohajeri A, Assadi H, Moazzeni M. Reconfiguration of the Molecular Sieve in MRU of Phase One Gas Refinery. Presented at the The second Symposium on Sustainnable Gas Production, Shiraz, Iran, 14-15 May 2013.
[23] Bárcia Silva PD. Separation of Light Naftha for the Octane Upgrading of Gasoline. Adsorption and Membrane Technologies and New Adsorbents 2010.

[24] Ferreira D, Magalhães R. Effective adsorption equilibrium isotherms and breakthroughs of water vapor and carbon dioxide on different adsorbents. Ind. Eng. Chem. Res. 2011;50: 10201-10210.
[25] Ryzhikov A, Hulea V, Tichit D, Leroi C, Anglerot D, Coq B. Methyl mercaptan and carbonyl sulfide traces removal through adsorption and catalysis on zeolites and layered double hydroxides. Appl. Catal. A 2011;397:218-224.
[26] Aspen Technology, Inc., Adsorption Reference Guide, Edited by United States of America, ed, 2001.
[27] Douglas KS, Ruthven M, Farooq S, Knaebel S. Pressure Swing Adsorption Wiley, 1993.
[28] Ruthven DM. Principles of Adsorption and Adsorption Process: John Wiley & Sons, 1984.
[29] Seader JD, Roper DK. Separation Process Principles, 3rd edition: Wiley, 2011.
[30] Perry RH, Green DW. Perry's Chemical Engineers Handbook, 7th Edition: McGraw-Hill, 1997.
[31] Suzuki M. Adsorption Engineering. Tokyo-Amsterdam: Elsevier, 1990.
[32] Asgari M, Anisi H, Mohammadi H, Sadighi S. Designing a commercial scale pressure swing adsorber for hydrogen purification. Pet. Coal 2014;56:552-561.
[33] Mokhatab S, Mak JY, Valappil V, Wood DA. Handbook of Liquefied Natural Gas: Gulf Professional Publishing, 2014.

*Corresponding author: sadighis@ripi.ir